

An SDR-based Turbo-SIC Implementation: Towards a 5G New Radio Advanced Receiver for Uplink Boosting

Milan Zivkovic, Juergen Otterbach, Marcos Tavares, Dale Harman, Dragan Samardzija
Nokia Bell Labs

Email: {milan.zivkovic, juergen.otterbach, marcos.tavares, dale.harman, dragan.samardzija}@nokia-bell-labs.com

Abstract—Significant uplink capacity improvements for the fifth generation (5G) wireless networks can be achieved by assigning the same time-frequency resources to several users simultaneously. Especially in the case of massive Machine-Type Communications (mMTC) for emerging Internet-of-Things (IoT) applications, where a very large number of devices must be provided with connectivity, the re-utilization of radio resources by concurrent transmissions from several devices is imperative for achieving economic viability. In this context, advanced signal processing in the evolved NodeB (eNB), namely multi-user detection (MUD), is a key enabler to reduce the mutual interference between users and appropriately decode the superposed signals. Turbo-SIC is a very efficient MUD scheme that applies successive interference cancellation (SIC), based on soft outputs of a turbo decoder. In this paper we introduce the implementation of an uplink Turbo-SIC receiver that follows the basic specifications of Long Term Evolution (LTE) systems. Using an LTE compliant open-source software defined radio (SDR) platform, named OpenAirInterface (OAI), we are able to show that Turbo-SIC offers several dBs of advantage over conventional receivers while its basic real-time processing requirements fit the capabilities of present general purpose processors (GPPs).

I. INTRODUCTION

The fifth generation (5G) of mobile networks, also named 5G New Radio (5G NR) within the 3GPP standardization, is foreseen to support a wide range of features and use cases to enable several new applications that go well beyond what is currently possible with Long Term Evolution (LTE) technology. Promising applications enabled by 5G NR include virtual/augmented reality, factory automation, massive cellular Internet of Things (IoT), and reliable remote operation of machines.

While the initial technology driver was the demand for very high data rates to support enhanced Mobile Broadband (eMBB) services, 5G NR will also be required to support Ultra-Reliable Low-Latency Communications (URLLC) and massive Machine-Type Communications (mMTC). Furthermore, 5G NR is expected to cover a wide range of the frequency spectrum, ranging from bands below 6 GHz to millimeter wave (mmWave) bands while being implementable over a multitude of network architectures, such as distributed/edge Cloud Radio Access Network (C-RAN), under the constraints of different backhaul and fronthaul latencies. Therefore, the major technical challenges of the 5G NR design is to enable aforementioned applications, which require Gbps data rates, low latencies (under 10 ms), high reliability, and the support for massive number of devices.

While the requirements mentioned above could be met by providing large amounts of spectrum, a more cost-effective solution can be achieved by assigning the same time-frequency resources to several users or data streams

simultaneously and providing reliable detection despite the introduced co-channel interference. In order to implement the solution above, advanced signal processing in the evolved NodeB (eNB), namely multi-user detection (MUD), is employed to reduce the mutual interference between users and appropriately decode the superimposed signals, therefore satisfying the required reliability. Typically, in 4G LTE networks, MUD is performed using linear receivers with multiple receive antennas, such as minimum mean square error (MMSE) [1] or interference rejection combining (IRC) [2] receivers, which treat all transmitted signals, except the signal from the desired user, as interferences. However, although MMSE and IRC receivers satisfy the needs of current applications, they are shown to be inefficient in future 5G scenarios, e.g., in a massive IoT where users experience highly correlated channels, or in the presence of heterogeneous QoS requirements, such as eMBB and URLLC traffic patterns in the same band.

In this context, Turbo-SIC is a very efficient MUD scheme that applies successive interference cancellation (SIC), based on soft outputs of turbo decoder. More specifically, Turbo-SIC is an advanced, non-linear receiver that iteratively enhances the detection reliability by using the estimation of previously detected users or streams to cancel their interference from the received signal. Due to its generality, Turbo-SIC can be employed in several scenarios, such as single-user (SU) and multi-user (MU) multiple-input multiple-output (MIMO), massive cellular IoT, eMBB, coordinated multipoint (CoMP) reception, and heterogeneous networks [3]. Moreover, Turbo-SIC is foreseen to enhance the performance of the proposed 5G NR non-orthogonal multiple access schemes, such as NOMA [4].

The concepts of iterative MUD have been studied for the last two decades [5][6][7]. More recently, those concepts have been applied to derive iterative multi-user receivers for LTE systems [8]. However, most of the work on iterative MUD was based on theoretical assumptions and idealized conditions or in PHY-layer only based laboratory setups, e.g., in [9]. Thereby, we take a further step towards validating Turbo-SIC for 5G NR applications.

Namely, we consider experimentation settings in which Turbo-SIC is fully integrated as a part of an LTE compliant system. The reason for the latter approach resides in the fact that 3GPP 5G NR specifications are not yet finished and, therefore, 5G equipment is not available for tests. Furthermore, the path towards 5G is seen more as a stepwise transition over 4.5G and 4.9G phases, rather than the introduction of a completely new air-interface [10].

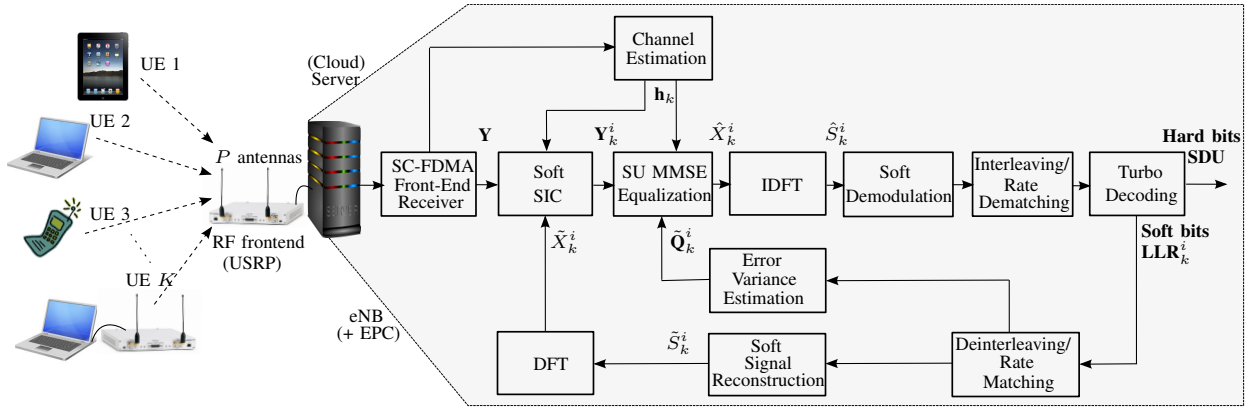


Fig. 1. LTE Uplink MIMO Turbo-SIC System.

However, the practical implementation of Turbo-SIC imposes several challenges, some of which will be discussed in this paper. As a very important both design and implementation issue, we address the very strict timing requirements for the receiver's processing in the eNB imposed by hybrid automatic repeat request (HARQ) protocol - a retransmission MAC protocol between eNB and UE. The timing requirements could potentially degrade the performance of the Turbo-SIC receiver because they limit the number of SIC iterations allowed to be performed in strictly predetermined time windows.

There are several software defined radio (SDR) based architectures that are considered in the scientific/developer/industrial research community for the design and performance assessment of 5G NR features, e.g., Amari LTE 100 [11], OpenLTE [12] and OpenAirInterface (OAI) [13]. However, to the best of the authors' knowledge, only the OAI framework presents the open source implementation of the entire LTE protocol, starting from the PHY-layer to the network level. OAI utilizes single instruction, multiple data (SIMD) intrinsics for parallel computing and contains multi-threaded implementations of eNB, User Equipment (UE) and Evolved Packet Core (EPC). Each of them can be interconnected with other LTE-compliant components, i.e., with a commercial eNB and EPC, and a commercial off-the-shelf (COTS) UEs.

In this paper, we introduce the implementation of a codeword-level Turbo-SIC receiver in OAI both to experimentally examine the Turbo-SIC detection performance in an LTE system and to evaluate processing requirements for real-time implementation on general purpose processors (GPPs). More specifically, to investigate the feasibility of practical implementation of Turbo-SIC in future 5G NR systems, we have modified the existing LTE-compliant single carrier frequency division multiple access (SC-FDMA) uplink eNB receiver in OAI to support detection of two UEs assigned to the same resource blocks in a multi-user-like scenario. Since the performed modifications are comprised only of standard compliant extensions in the eNB receiver and MAC scheduler, they allow for fully interoperability with standard LTE COTS UE devices. Moreover, our implementation can be further generalized to several collocated UEs, as well as, extended to other scenarios such as NOMA and CoMP joint reception, where two edge UEs communicate to two backhauled eNBs.

The remainder of this paper is organized as follows.

Section II introduces the uplink MIMO system model with Turbo-SIC detection and addresses the limiting factor of HARQ timing requirements. In Section III, we introduce the modifications of the LTE-compliant eNB receiver in OAI to enable Turbo-SIC detection. Simulation results and computational complexity analysis are presented in Section IV. Finally, some concluding remarks are given in Section V.

II. UPLINK SYSTEM MODEL

A. Multi-user detection (MUD)

A high level model of multi-user MIMO with Turbo-SIC receiver for the LTE uplink is shown in Fig. 1. In this scenario, a total of K users, each equipped with one antenna, occupy the same time-frequency resources, i.e., they transmit the service data units (SDU) transport block codewords over the same physical resource blocks (PRBs) in the same subframes. In the eNB receiver, equipped with P receive antennas, after the FFT operation in SC-FDMA front-end receiver, the frequency-domain received signal $\mathbf{Y} = [Y_1, \dots, Y_P]^T$ per subcarrier (throughout this paper, subcarrier indices are omitted for the sake of clarity) is given by:

$$\begin{aligned} \mathbf{Y} &= \mathbf{H}\mathbf{X} + \mathbf{N}, \\ &= \sum_{k=1}^K \mathbf{h}_k X_k + \mathbf{N}, \end{aligned} \quad (1)$$

where $\mathbf{X} = [X_1, \dots, X_K]^T$ is the vector containing transmitted complex symbols X_k , for $k = 1, \dots, K$, $\mathbf{N} = [N_1, \dots, N_P]^T$ is the circularly symmetric complex AWGN vector with variance $E\{N_p N_p^* \} = \sigma^2$, for $p = 1, \dots, P$, and

$$\mathbf{H} = [\mathbf{h}_1, \dots, \mathbf{h}_K] \quad (2)$$

is the $P \times K$ channel matrix. Here, $\mathbf{h}_k = [h_{1k}, \dots, h_{Pk}]^T$, for $k = 1, \dots, K$, denotes the k th column vector of the channel matrix \mathbf{H} , i.e., it contains the channel coefficients h_{pk} between the UE k and eNB receive antennas p .

The optimal detection scheme for MIMO systems can be derived from maximum likelihood (ML) and maximum *a posteriori* probability (MAP) criteria. However, those optimal detection schemes are characterized by exponentially increasing complexity with respect to the modulation order and number of transmit antennas [7]. Therefore, in practical systems, several suboptimal methods are considered, such as linear detectors and equalization based on interference cancellation.

Due to their relatively low computational complexity, the most commonly used detectors are based on linear equalization, such as zero forcing (ZF) and MMSE. The

linear detectors treat all of transmitted signals as interferences except the signal from the desired user. To detect the signal of the desired user, the received vector \mathbf{Y} is filtered to minimize the influence of other interfering users. The estimated signal can be then written as

$$\hat{\mathbf{X}} = \mathbf{W}\mathbf{Y}, \quad (3)$$

where \mathbf{W} is $K \times P$ filter matrix derived according to the linear detector's criterion.

In the following, we introduce the MMSE equalizer as the basic building block for the Turbo-SIC receiver.

B. MMSE detection

The MMSE detector minimizes the mean squared error between the actually transmitted symbol and the output of the linear detector, i.e., the MMSE filter matrix \mathbf{W}_{MMSE} is derived according to

$$\begin{aligned} \mathbf{W}_{MMSE} &= \arg \min_{\mathbf{W}} \mathbb{E}\{|\mathbf{X} - \mathbf{W}\mathbf{Y}|^2\}, \\ &= \mathbf{H}^H \mathbf{V}, \\ &= \mathbf{H}^H (\mathbf{H}\mathbf{H}^H + \sigma^2 \mathbf{I}_P)^{-1}, \end{aligned} \quad (4)$$

where \mathbf{I}_P is the $P \times P$ identity matrix and the channel inversion matrix \mathbf{V} is given by

$$\mathbf{V} = (\mathbf{H}\mathbf{H}^H + \sigma^2 \mathbf{I}_P)^{-1}. \quad (5)$$

The estimated frequency domain symbol of the k th user after single-user MMSE (SU MMSE) equalization becomes

$$\begin{aligned} \hat{X}_k &= \mathbf{w}_k \mathbf{Y}, \\ &= \mathbf{h}_k^H (\mathbf{H}\mathbf{H}^H + \sigma^2 \mathbf{I}_P)^{-1} \mathbf{Y}, \end{aligned} \quad (6)$$

where \mathbf{w}_k is the k th row vector of the filter matrix \mathbf{W}_{MMSE} .

The MMSE detector's implementation is of relatively low complexity. However, it offers only limited performance in spatially correlated channels due to high level of residual interference still present after the detection. This is especially critical in massive cellular IoT where the number of users is much greater than the number of received antennas. The performance of linear detectors can be improved by iteratively enhancing the reliability of the data estimates for each SDU by using an estimation of previously detected symbols to cancel their interference from the received signal. In this interference cancellation-based algorithm, named Turbo-SIC, the MMSE equalizer and turbo decoder jointly operate in an iterative loop benefiting from mutual information exchange, as shown in Fig. 1.

C. Turbo-SIC detection

The first step in Turbo-SIC is to order SDUs of different UEs in such a way that the one with the best chances to be correctly decoded is processed first. The log-likelihood ratios (LLRs) at the output of the turbo decoder are used to reconstruct QAM symbols and get soft estimates of each of the transmitted SDUs and of the variance of the residual interference. These soft-estimates are fed back to an interference canceller that progressively remove the mutual interference contribution. In the next step, the SU MMSE receiver is applied to the signal with the reduced interference to decode the corresponding SDU. The operations of reconstructing the previous streams in the feedback, cancelling the interference and applying the SU MMSE receiver to decode the current SDU constitutes a Turbo-SIC equalization iteration. The number of iterations depends on the system design and on the available processing times determined by HARQ requirements.

Let's now consider the i th Turbo-SIC iteration. The equivalent channel gain of the k th SDU, named \hat{h}_k^i , can be expressed as:

$$\hat{h}_k^i = \mathbb{E}\{\mathbf{h}_k^H (\mathbf{H}\mathbf{H}^H + \sigma^2 \mathbf{I}_P)^{-1} \mathbf{h}_k\}, \quad (7)$$

where $\mathbb{E}\{\cdot\}$ presents the averaging over all occupied sub-carriers. After the detection of the user with the greatest \hat{h}_k^i , the corresponding SDU is reconstructed by means of soft modulation and fed back to the interference canceller.

The signal of the user k (or k th SDU) in the i th iteration after cancellation of all interfering users becomes

$$\mathbf{Y}_k^i = \mathbf{h}_k X_k + \sum_{l=1, l \neq k}^K \mathbf{h}_k (X_l - \tilde{X}_l^i) + \mathbf{N}, \quad (8)$$

where \tilde{X}_l^i is the soft modulated reconstructed symbol of the user l in the i th iteration.

From (8), the SU MMSE receiver computes an MMSE estimate of the symbols, based on received samples with reduced interference. The signal estimates after SU MMSE equalization is given by

$$\hat{X}_k^i = \mathbf{w}_k^i \mathbf{Y}_k^i, \quad (9)$$

with

$$\begin{aligned} \mathbf{w}_k^i &= \mathbf{h}_k^H \mathbf{V}_k^i \\ &= \mathbf{h}_k^H (\mathbf{H}\tilde{\mathbf{Q}}_k^i \mathbf{H}^H + \sigma^2 \mathbf{I}_P)^{-1}, \end{aligned} \quad (10)$$

where $\mathbf{V}_k^i = (\mathbf{H}\tilde{\mathbf{Q}}_k^i \mathbf{H}^H + \sigma^2 \mathbf{I}_P)^{-1}$ is the channel inversion matrix for the k th user in the i th iteration. Here, $\tilde{\mathbf{Q}}_k^i = \mathbf{diag}[\tilde{q}_{k,1}^i, \dots, \tilde{q}_{k,K}^i]$ is the $K \times K$ diagonal matrix of the residual interference powers in the i th iteration, where its l th element can be expressed as

$$\tilde{q}_{k,l}^i = \begin{cases} 1, & l = k \\ \mathbb{E}\{|X_l - \tilde{X}_l^i|^2\}, & l \neq k, \text{NACK}_l^i \\ 0, & l \neq k, \text{ACK}_l^i \end{cases}. \quad (11)$$

Note that in the very first iteration $i = 1$, $\mathbf{V}_{k_{\max}}^1 = \mathbf{V}$, for $k_{\max} = \max_k \hat{h}_k^1$, i.e., $\tilde{\mathbf{Q}}_{k_{\max}}^1$ is the identity matrix \mathbf{I}_K .

Depending on whether the codeword l is correctly decoded in the i th iteration, i.e., whether NACK_l^i or ACK_l^i is derived from the output of CRC check of the Turbo decoder, there are two ways to reconstruct the decoded signal \tilde{X}_l^i and calculate the corresponding variance of the residual interference $\tilde{q}_{k,l}^i$. If the CRC check of the turbo decoder is ACK_l^i , the hard bits from the turbo decoder output can be directly mapped to QAM symbols and $\tilde{q}_{k,l}^i$ becomes zero as the signal can be perfectly reconstructed. In the case when the turbo decoder outputs NACK_l^i , the signal and interference variance can be computed using the the LLRs from the turbo decoders output. Low complexity analytical methods for computation of the soft reconstructed signal and can be found in literature, e.g., in [14]. Moreover, the residual interference variance, i.e., the elements of $\tilde{\mathbf{Q}}_k^i$, can be computed using second order statistics, where the complexity increases with the constellation size, or using low-complexity analytical approximations [3].

D. Timing requirements in LTE FDD

Due to its iterative nature, Turbo-SIC detection may result in increase processing times in the eNB. However, in LTE-FDD networks, very strict timing requirements for the receiver's processing in the eNB are imposed by HARQ.

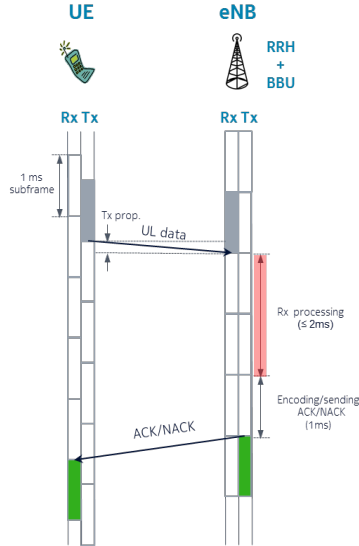


Fig. 2. HARQ process timing requirements.

The transmission time interval (TTI) of an LTE time unit, i.e., a subframe, is equal to 1 ms. Within this timing granularity, the HARQ processes regulate the data retransmission between UE and eNB by reporting the reception status of each received subframe back to the transmitter. More specifically, it takes 8 ms for a single HARQ process to send data, receive NACK or ACK, and, finally, retransmit the previously sent information or transmit a new chunk of data, respectively. Fig. 2 exemplifies and shows the timing requirements of a HARQ process for an uplink transmission.

In the case of the (eNB) receiver processing requirements, each SDU packed received at subframe k has to be reported through an ACK/NACK at the subframe $k + 4$. Therefore, the total eNB processing time is 3 ms, where 2 ms, i.e., two subframes, are used for SDU decoding and 1 ms, i.e., one subframe, for scheduling and ACK/NACK encoding. Then, at the (UE) transmitter, the ACK/NACK message has to be decoded before assembling subframe $k + 8$.

Therefore, the number of the iterations of Turbo-SIC is determined such that the complete receive PHY-layer processing should fit in 2 ms. Since processing times differ depending on the occupied bandwidth, used modulation and coding scheme (MCS) and the number of resource blocks, the Turbo-SIC receiver design should take in consideration different choices of these system parameters.

III. TURBO-SIC IMPLEMENTATION IN OAI

A. OpenAirInterface (OAI)

The core of OAI is a real-time software modem written in standard C. The implementation contains Streamed SIMD Extension (SSE) and advanced vector extensions (AVX) intrinsics for some of the time-intensive operations, such as channel estimation, FFT/IFFT, equalization, turbo encoding and decoding, and preferably runs on a low latency kernel. OAI can operate in several modes which accelerates the design and implementation in a systematic way. The first mode is an unitary (link level) simulation - *unisim*, where different LTE physical channels (PUSCH, PDSCH, PRACH, PDCCH, PUCCH) and features can be tested before integrating with higher layers. Furthermore, OAI can run as an

emulation environment - *oisim* with or without PHY-layer abstractions, which enables investigation of system level features [15]. Finally, OAI operates as a real-time modem - *lte-softmodem*, interfaced with an RF platform, such as Universal Software Radio Peripheral (USRP) [16], which enables over-the-air LTE-compliant operation and interfacing with EPC, while satisfying the given timing requirements.

As an initial implementation step, while introducing the new Turbo-SIC functionality into the existing OAI eNB software modem, we have investigated the performance of the implemented features on link level simulations, i.e., by means of achievable gains in BLER vs. SNR performance. Since we are focusing on enhancing uplink LTE features, the integration of Turbo-SIC only requires modifications on the eNB receiver, MAC scheduler and content of Downlink Control Information (DCI) 0 message containing uplink scheduling grants.

B. MMSE receiver

MMSE detection is the basic receiver for a single Turbo-SIC iteration, as shown in Fig. 1. In this context, as an initial step, we have implemented the OAI multi-user MMSE receiver, as shown in Fig. 3, for the case of two UEs. The *ofdm_demod()* block is a generic OAI block performing pre-FFT operation, noise power estimation, and FFT operation. The common processing for both UEs is done in *ulsch_preproc()*, where the first step is to extract the scheduled PRBs producing both received frequency-domain symbols \mathbf{Y} and demodulation reference symbols (DMRS).

The channel estimation, performed in *mu_channel_estimation()*, is based on multi-user (MU) least squares (LS) channel estimation, widely investigated in literature [17][18]. Since both UEs occupy the same PRBs, each DMRS is scheduled with different cyclic shifts, to separate the LS channel estimates in time domain. The assignment of different DMRS cyclic shifts for different UEs is a part of the scheduling grant message in DCI 0, issued by MAC scheduler at eNB.

After obtaining the channel estimates \mathbf{H} , the channel inversion matrix \mathbf{V} , given in (5), is calculated in *mmse_channel_inversion()*. Based on \mathbf{Y} , \mathbf{V} and \mathbf{H} , the user-specific processing is done in *ulsch_demod_su()*, where the SU MMSE equalization, given in (6), is performed in *su_mmse_equalizer()*. Furthermore, generic OAI blocks are used to perform IDFT, soft demodulation, and decoding of each user's SDU.

C. Turbo-SIC receiver

The OAI Turbo-SIC receiver is shown in Fig. 4 for the case of two UEs. The first step in Turbo-SIC processing is to order SDUs of different UEs in such a way that the one with the best chances to be correctly decoded is processed first, as described in Subsection II-C. This is done by calculating the equivalent channel gain \hat{h}_k^i , given in (7), which is performed in *mmse_channel_inversion()*. In the first iteration, the UE with the highest \hat{h}_k^i , e.g., UE 1, as shown in Fig. 4, is further processed using SU MMSE detection, as described above. The way of how the detection of (weaker) UE 2 will be further performed depends on the CRC check output of turbo decoder for UE 1, obtained in *ulsch_decoding_sic()*.

If the CRC check produces ACK, i.e., the SDU of UE 1 is perfectly reconstructed, the hard bits from the

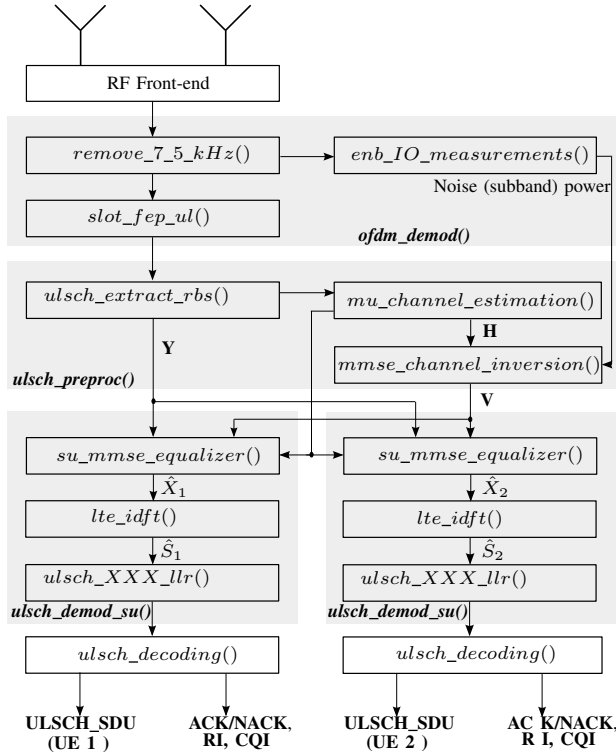


Fig. 3. OAI multi-user MMSE receiver.

turbo decoder output $\hat{\mathbf{b}}_1^1 = \mathbf{b}_1^1$ are directly encoded and modulated to QAM symbols \hat{X}_1^1 . This is done by directly feeding the decoded UE 1 SDU to the generic OAI *lte_segmentation()* block in *ulsch_encoding_sic()*, a modified generic OAI encoding block, shown in Fig. 5. As given in (11), the residual interference power of UE 1 in the first iteration then becomes zero and is further fed to *mmse_channel_inversion()* in *ulsch_sic()*.

On the other hand, if the turbo detector outputs NACK, the SDU of UE 1 can not be perfectly reconstructed for the detection of UE 2. In this case, soft outputs of the turbo decoder LLR 1 are deinterleaved and rate matched in *ulsch_decoding_sic()*, producing $\hat{\mathbf{f}}_1^1$, which is further fed to data and control multiplexing in *ulsch_encoding_sic()*, as shown in Fig. 5, and further modulated to soft QAM symbols \hat{X}_1^1 . The corresponding residual interference power of UE 1 in the first iteration $\tilde{q}_{2,1}^1$ is then different from zero, calculated as in (11), and fed to *mmse_channel_inversion()* in *ulsch_sic()*.

Prior to the detection of UE 2, the reconstructed signal \hat{X}_1^1 is cancelled from the original received signal \mathbf{Y} in *ulsch_sic_compensation()*, as given in (8). The “interference-free” symbol \mathbf{Y}_2^1 is fed to *su_mmse_equalizer()*, together with the channel inverse matrix \mathbf{V}_2^1 and further processed to decode the SDU of UE 2, finalizing the first Turbo-SIC iteration. Similarly, to further proceed to the next Turbo-SIC iteration and the detection of UE 1, the UE 2 is reconstructed based on its ACK/NACK, subtracted from the original signal \mathbf{Y} and fed to SU MMSE equalizer, which takes as input the residual interference power of UE 2 according to equation (11). The iterative process continues until all users are successfully decoded or a maximum number of iterations is reached.

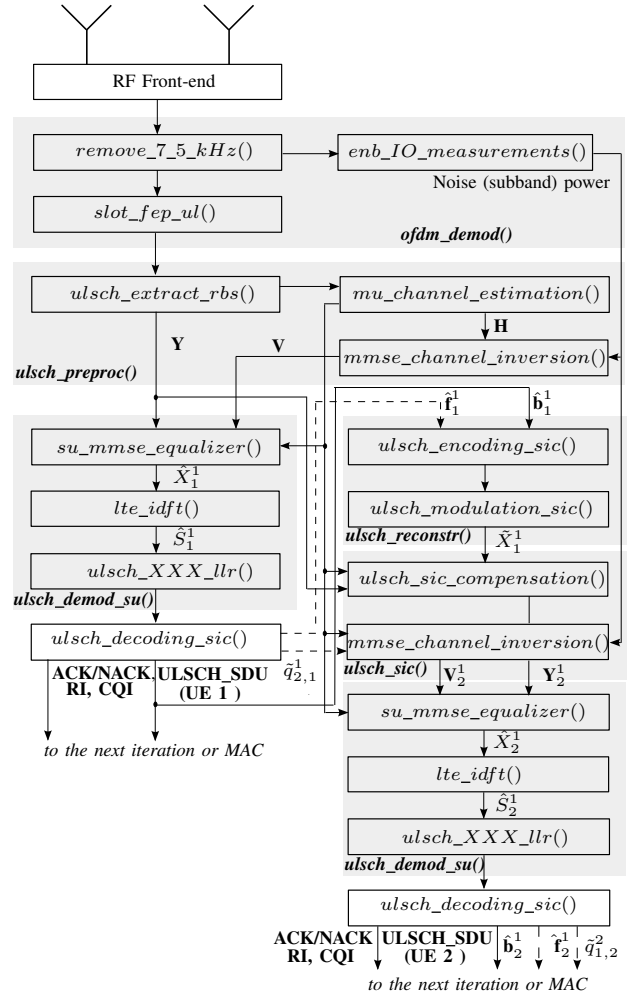


Fig. 4. OAI multi-user Turbo-SIC receiver (with one iteration).

IV. RESULTS

A. Simulation results

The performance of the LTE-compliant implementation of Turbo-SIC in OAI is evaluated in a unitary link-level OAI simulator *unisim* that is utilized for testing LTE physical channels and features before integration with higher layers in the real-time *lte-softmodem*, which is interfaced with USRP. More specifically, Physical Uplink Shared Channel (PUSCH) simulator *ulsim* is modified to enable the evaluation of a scenario having two UEs with single transmit antennas, each sending a single SDU over the same physical resource blocks (PRBs) to the common eNB equipped with two receive antennas over uncorrelated frequency-selective Rayleigh channels.

The simulations are performed on a general purpose computer equipped with Intel XEON E5-2637 v3 @3.5 GHz with OAI operating in Ubuntu 14.04 with *3.19.0-61-lowlatency* kernel. The average block error rate (BLER) of both UEs is used as a metric to evaluate the performance of the Turbo-SIC receiver with one iteration and to compare against the performance of the MMSE receiver, which is the basic linear detector for each Turbo-SIC iteration, as discussed in Section II. In this context, the maximum number of the iterations in turbo decoder is four. The average signal-to-noise ration

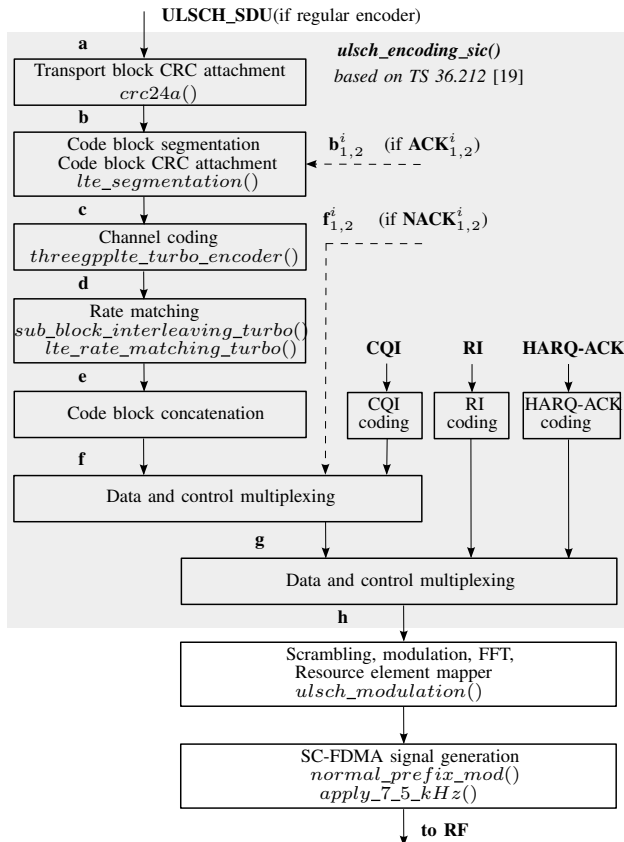


Fig. 5. OAI PUSCH modulation.

(SNR) is equal for both UEs and ranges from -5 to 30 dB. Two simulation scenarios are considered: Turbo-SIC and MMSE with perfect channel estimation, and with MU LS channel estimation, which are shown in Fig. 6 and Fig. 7, respectively. The performances are evaluated for SDU occupying 25 PRBs (5 MHz) for three MCSs that correspond to the coding rate of 1/2 for different modulation schemes, i.e., MCS: 8, 15, and 21 for QPSK, 16-QAM and 64-QAM, respectively.

Both figures show the significant performance gain of the implemented receiver with one Turbo-SIC iteration compared to the linear MMSE receiver. More specifically, at BLER = 10%, SNR gains for MCS 8, 15, and 21 are ≈ 4 , ≈ 3 and ≈ 2 dB, respectively. The performance gap between Turbo-SIC and MMSE receivers is expected to further increase if more Turbo-SIC iterations are allowed. Moreover, by comparing curves in Fig. 6 and Fig. 7, it can be seen that the influence of MU LS channel estimation, described in Section III causes the 2 – 3 dB performance loss compared to ideal receiver case.

B. Processing times

To evaluate the timing requirements of the Turbo-SIC receiver we inspect the processing delays of the OAI implementation in uplink eNB processing. This analysis can be beneficial for the following reasons. Primarily, by profiling the processing times of the LTE PHY-layer with 2-user Turbo-SIC detection in the eNB receiver, it is possible to get a better understanding about the feasibility and practical constraints of implementing Turbo-SIC on GPP platforms, such as OAI. Furthermore, the analysis enables the identification of potential improvements and performance limits due to the strict

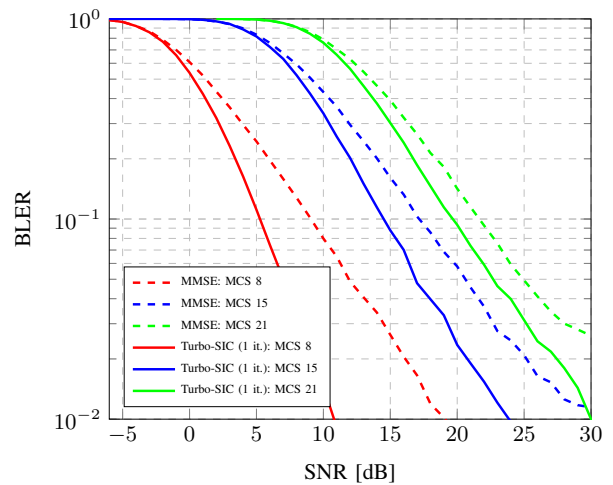


Fig. 6. BLER vs SNR performance in in frequency selective Rayleigh fading channel with perfect channel estimation.

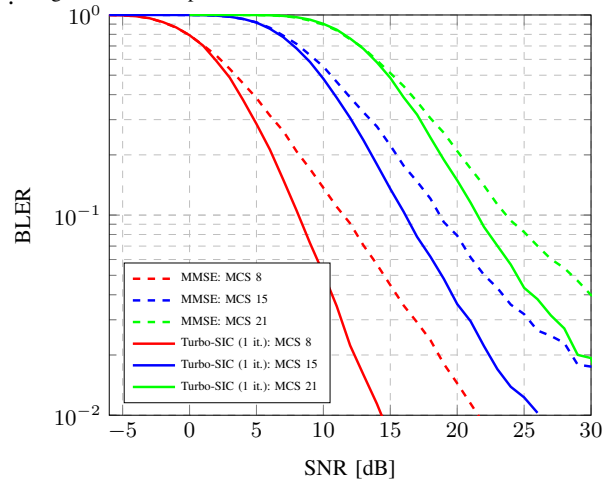


Fig. 7. BLER vs SNR performance in frequency selective Rayleigh fading channel with MU LS channel estimation.

HARQ timing constraints, addressed in Subsection II-D.

We use the *ulsim* simulator with the same system parameters as defined in previous subsection. The investigation is performed at SNR of 30 dB, which limits the processing time variation of the turbo decoder [20]. The execution times of each time processing module is derived using the *RDTSC* instruction available for all x86/x64 processors, by comparing timestamps at the beginning and at the end of computing. More specifically, *RDTSC* counts the number of CPU clocks between the beginning and the end of the computing in each block. Fig. 8 shows the total processing times of SU maximum ratio combining (MRC), MMSE and one-iteration Turbo-SIC receiver for MCS: 8, 15, and 21. Two cases of occupied bandwidths with full PRBs allocation for two UEs are considered: 5 MHz (25 PRBs) and 20 MHz (100 PRBs). Full PRBs allocation means the maximum load for the occupied bandwidth. It is noticeable that three critical parameters, the number of PRBs, MCS indices and radio bandwidth influence the required processing times. By comparing the two considered loads, it is shown that for each MCS, the processing times differ by a factor four.

Moreover, compared to single user MRC, the MMSE receiver requires more than double processing times, i.e., 2.45 for MCS = 8, and 2.25 for MCS = 15 and MCS = 21. It is shown that each new Turbo-

TABLE I
AVERAGE RECEIVE PROCESSING TIME PER SUBFRAME AT ENB WITH 2 RECEIVE ANTENNAS AND MULTI-USER DETECTION GIVEN FULL PRB ALLOCATION AT 5MHZ.

Processing time	MRC (single user) [μ s]	MRC [μ s]	MMSE [μ s]	Turbo-SIC (1. iter.) [μ s]
Total Rx PHY MCS = 8 / 15 / 21	166.4 / 255.8 / 354.5	336.1 / 510.2 / 720.3	405.2 / 573.3 / 798.6	534.2 / 739.3 / 1003.1
<i>ofdm_demod</i>	34.3	34.9	33.9	33.9
<i>ulsch_preproc()</i> :				
<i>su/mu_channel_estimation()</i>	21	69.7	136.8	136.5
+ <i>mmse_channel_inversion()</i>	21	69.7	69.7	70.160.4
+ <i>mmse_channel_inversion()</i>	---	---	64.1	60.4
<i>ulsch_demod_SU</i>	28.3	56.6	69.3	68.4
<i>ulsch_decoding</i>	82.6/170/265.7	164.1/340.1/550.1	164.3/334.1/549.1	167.4/334.9/549
<i>ulsch_reconstr</i>	---	---	---	64.8/103.2/144
<i>ulsch_SIC_compensation</i>	---	---	---	62.7

iteration (signal reconstruction and SIC compensation) add additional 30% of the processing time, compared to the MMSE receiver. This can be further used to predict the number of allowed Turbo iterations based on available processing times, given the number of PRBs, MCS and occupied bandwidth.

Further timing profiling of the implemented 2-users Turbo-SIC receiver with one iteration and its comparison against SU MRC, 2-users MRC and 2-users MMSE at 5 MHz is shown in Table I. It can be seen that non-user specific processing blocks in the eNB, i.e., time-domain processing (pre FFT, FFT and noise power estimation) in *ofdm_demod()*, and MU channel estimation with initial user ordering and channel inversion matrix computation in *ulsch_preproc()*, jointly occupy only $\approx 31.8\%$, $\approx 23\%$, $\approx 17\%$ of the total processing time, for MCS = 8, MCS = 15 and MCS = 21, respectively, while being performed only once, prior to the first iteration. This suggests that the rest of the processing time goes to users' detection, signal reconstruction and cancellation, i.e., to the operations that are repeated at each Turbo-SIC iteration and therefore affect the overall processing budget.

V. CONCLUSION

We have introduced the implementation of a codeword-level Turbo-SIC receiver in OAI, an LTE-compliant open-source SDR platform. To investigate the feasibility of practical implementation of Turbo-SIC in future 5G NR systems, we have modified the existing LTE-compliant uplink eNB receiver in OAI to support detection of two UEs assigned to the same resource blocks. We have evaluated the performance of the given receiver and examined the processing requirements for

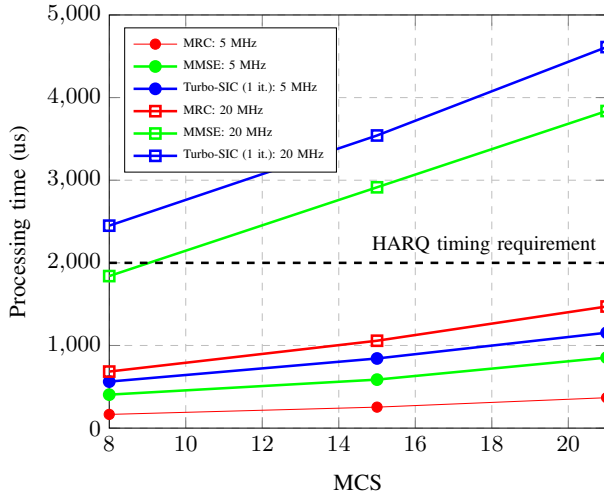


Fig. 8. eNB processing time for receiving packets given full PRB allocation at 5 MHz and 20 MHz on an Intel XEON E5-2637 v3 @ 3.5 GHz.

real-time implementation on GPPs. This implementation can be further generalized to several collocated UEs as well as extended to other scenarios such as NOMA and CoMP joint reception. As a next step, we plan to conduct over-the-air experiments to examine the real-time performance of the implemented Turbo-SIC receiver in an RF environment. Moreover, to achieve the full performance gain offered by Turbo-SIC, several more advanced scheduling techniques involving HARQ retransmission are currently under investigation.

REFERENCES

- [1] P. W. Wolniansky, G. J. Foschini, G. D. Golden, and R. A. Valenzuela, "V-BLAST: an architecture for realizing very high data rates over the rich-scattering wireless channel," in *Proc. of IEEE ISSSE*, Sep 1998, pp. 295–300.
- [2] Y. Leost, M. Abdi, R. Richter, and M. Jeschke, "Interference rejection combining in LTE networks," *Bell Labs Tech. J.*, vol. 17, no. 1, pp. 25–49, June 2012.
- [3] M. Tavares, D. Harman, M. Zivkovic, J. Otterbach, and D. Samardzija, "Successive interference cancellation and multi-user minimum mean square channel estimation based on soft decoding information," U.S. Patent, Filled, March 2017.
- [4] X. Wei, H. Liu, Z. Geng, K. Zheng, R. Xu, Y. Liu, and P. Chen, "Software defined radio implementation of a non-orthogonal multiple access system towards 5G," *IEEE Access*, vol. 4, pp. 9604–9613, 2016.
- [5] H. V. Poor, "Turbo multiuser detection: A primer," *J. of Commun. and Netw.*, vol. 3, no. 3, pp. 1–6, Sept 2001.
- [6] G. Yue, N. Prasad, and S. Rangarajan, "Iterative MMSE-SIC receiver with low-complexity soft symbol and residual interference estimations," in *Proc. of ACSSC*, Nov 2013, pp. 2113–2117.
- [7] R. E. Chall, F. Nouvel, M. Hélar, and M. Liu, "Iterative receivers combining MIMO detection with turbo decoding: performance-complexity trade-offs," *EURASIP J. Wirel. Commun. Netw.*, no. 1, p. 69, 2015.
- [8] G. Berardinelli, C. N. Manchon, L. Deneire, T. B. Sorensen, P. Mogensen, and K. Pajukoski, "Turbo receivers for single user MIMO LTE-A uplink," in *Proc. of IEEE VTC Spring 2009*, 2009, pp. 1–5.
- [9] A. Purkovic and M. Yan, "Turbo equalization in an LTE uplink MIMO receiver," in *Proc. of MILCOM 2011*, Nov 2011, pp. 489–494.
- [10] *The path to 5G: New services with 4.5G, 4.5G Pro and 4.9G*, Nokia Whitepaper, 2017. [Online]. Available: https://pages.nokia.com/2198.Path_To_5G.html
- [11] "Amari LTE." [Online]. Available: <https://www.amarisoft.com>
- [12] "OpenLTE." [Online]. Available: <http://openlte.sourceforge.net/>
- [13] "OpenAirInterface." [Online]. Available: <http://www.openairinterface.org>
- [14] L. Fang, Q. Guo, D. Huang, and S. Nordholm, "A low cost soft mapper for turbo equalization with high order modulation," in *Proc. of ISOCC 2012*, Nov 2012, pp. 305–308.
- [15] A. Virdis, N. Iardella, G. Stea, and D. Sabella, "Performance analysis of OpenAirInterface system emulation," in *Proc. of FiCloud 2015*, Aug 2015, pp. 662–669.
- [16] "USRP." [Online]. Available: <http://www.ettus.com>
- [17] X. Hou, Z. Zhang, and H. Kayama, "DMRS Design and Channel Estimation for LTE-Advanced MIMO Uplink," in *Proc. of IEEE VTC 2009 Fall*, Sept 2009, pp. 1–5.
- [18] M. Jiang, G. Yue, N. Prasad, and S. Rangarajan, "Enhanced DFT-based channel estimation for LTE uplink," in *Proc. of IEEE VTC 2012 Spring*, May 2012, pp. 1–5.
- [19] 3GPP TS 36.212, "Evolved Universal Terrestrial Radio Access (E-UTRA): Multiplexing and channel coding," ETSI, Standard.
- [20] N. Nikaein, "Processing radio access network functions in the cloud: Critical issues and modeling," in *Proc. of MCCS 2015*, ser. MCS '15. New York, NY, USA: ACM, 2015, pp. 36–43.